Na and Hyung *Int J Concr Struct Mater* (2024) 18:49
https://doi.org/10.1186/s40069-024-00689-6

International Journal of Concrete Structures and Materials

REVIEW

Open Access

Investigation of Applicability of Non-sintered Cement Mortar for Precast Concrete by Steam Curing

Hyeong-Won Na[1] and Won-Gil Hyung[2*]

Abstract

Non-sintered cement (NSC) mortar was developed using only industrial by-products, such as ground granulated blast furnace slag, classes C and F fly ashes, and slaked lime. The characteristics of different NSC mortar formulations were investigated, as well as their applicability for use in forming precast concrete products. X-ray diffraction and scanning electron microscope analyses were performed to examine the internal structure of the different formulations. Overall, the developed NSC mortar satisfied the existing quality standards in terms of strength performance and absorption rate. Therefore, it is expected to be highly applicable as a raw material for production of the desired cement products.

Keywords Blast furnace slag, Fly ash, Non-sintered cement, Precast concrete

1 Introduction

Global warming is currently one of the biggest threats to the human race. The 2019 UN Climate Action Summit called for full-fledged "action" from countries worldwide toward the implementation of the Paris Agreement from 2020 onward. Consequently, approximately 65 countries have committed to achieving net-zero greenhouse gas (GHG) emissions by 2050. To this end, specific measures must also be implemented toward the transition to a sustainable construction industry.

In 2017, domestic industrial process emissions totaled 56.0 million tons of CO_2eq in South Korea (7.9% of the country's total emissions), of which mineral industry emissions amounted to 36.5 million tons of CO_2eq (65.2% of the industrial process emissions). In the domestic mineral industry, GHG emission results from the production of ordinary Portland cement (OPC) and lime, as well as the production and consumption of soda ash. Specifically, CO_2 is discharged as part of a decarbonation reaction to calcine raw materials containing carbonates. Hence, the resulting emissions continually increase in proportion to cement production. Meanwhile, the domestic GHG reduction target has risen from 30% in the year 2009 to 37% in 2015 (Korea Ministry of Environment, 2019). Additionally, the demand for non-sintered cement (NSC) produced using industrial by-products is expected to increase gradually under the 2015 Emission Trading System and the enforcement of the 2019 Framework Act on Resources Circulation. Particularly, different mixing proportions and curing temperatures of binders are being examined domestically and internationally in view of the use of ground granulated blast furnace slag (GGBFS) and fly ash (FA).

GGBFS contains sufficient reactive Si, Al, and Ca, which can be blended with raw aluminosilicate materials to enhance alkaline reactivity (Shin, 2020). Moreover, it reacts with alkaline activators to form calcium silicate hydrate (CSH) hydration products similar to OPC.

Journal information: ISSN 1976-0485 / eISSN 2234-1315.

*Correspondence:
Won-Gil Hyung
beda@yu.ac.kr
[1] Post Doctor, School of Architectural Engineering, YeungNam University, 280 Daehak-ro, Gyeongsan-si, Gyeongsangbuk-do, Korea
[2] Professor, School of Architecture, Yeungnam University, 280 Daehak-ro, Gyeongsan-si, Gyeongsangbuk-do, Korea

Class F fly ash (FFA) is used as a major admixture, and its high aluminosilicate content and spherical particles improve workability. Class C fly ash (CFA), when used as an admixture, may cause loss of fluidity and cracking because it contains components such as CaO and SO_3 that cause initial heat generation and expansion (Lee, 2017). Hence, the Korean Standard (KS L 5405) recommends using a mix of CFA and FFA for qualitative manufacturing (Korean Agency for Technology and Standards Homepage, 2023).

Studies on the utilization of industrial by-products mainly concern binders that use alkaline activators. Additionally, with increasing environmental concerns, these studies tend to focus on commercialization by examining the characteristics according to the type and usage of raw materials and activators. Although alkaline activators tend to be used for improving the GGBFS response, additional operations must be minimized during manufacturing. Furthermore, economic feasibility must be ensured to increase the usability of non-sintered binders.

Therefore, this study aims to investigate the applicability of NSC mortar, which utilizes industrial by-products, without relying on alkaline activators for developing concrete products. The proposed NSC mortar is expected to contribute to environmental load reduction, support the expansion of industrial by-product usability, and achieve quality stability through optimal mixtures and efficient solutions.

2 Materials and Methods

2.1 Materials

Table 1 shows the chemical compositions of the NSC mortar materials. This study aimed to use 100% industrial by-products and 0% alkaline activators and OPC.

The cements used in the experiments were OPC, which meets the standards of KS L 5201 (Type I) Portland cement, and GGBFS, which meets the standards of KS F 2563 GGBFS for concrete. GGBFS is typically used as a base material, and CFA has been substituted as a stimulant to promote GGBFS hydration reactions owing to its latent hydraulic property. To complement the soundness of CFA, we mixed it with FFA to realize a suitable mixing proportion involving three different substitution ratios (CFA:FFA = 1:3, 1:1, and 3:1). The applicability of slaked lime (SL) was also examined to complement the strong alkalinity of the mixture. Figure 1 shows the particle shape of the material.

2.2 Production of Specimens

Table 2 shows the mixing proportions of the NSC mortar specimens. This was derived through basic experiments. As a result of selecting GGBFS as the base material and using OPC and CFA as stimulus materials, the bending strength was found to be so low that it could not be measured if OPC was not used. And when more than 20% of CFA was used, the compressive strength rapidly decreased. Therefore, CFA was used as a stimulus material that can replace OPC, and the substitution ratio was set to 20% or less. Additionally, when using a mixture of GGBFS and CFA, FFA was replaced for the purpose of reducing W/B and improving the stability of the binder.

The weight proportion of binder materials to fine aggregates (B:S) was set to 1:3, and the water–binder ratio (W/B) was fixed at 40%. B:S was set to 1:3 as specified in KS L ISO 679 Cement-Testing Method-Strength Measurement, and W/B was set based on Flow 0 mm in consideration of factory production.

The NSC mortar was blended and mixed with water after the raw materials were weighed, and the specimens were developed using a three-gang mold (40 × 40 × 160 mm). The specimens were steam cured (temperature 60 ± 5 ℃; relative humidity 100%) one hour after pre-curing. During the steam curing, the specimens were maintained at the highest temperature (60 ± 5 ℃) for 5 h, heaped-up for 2 h, and slowly cooled afterward.

2.3 Experimental Methods

Table 3 shows the KS for precast concrete (PC) products. Based on this standard, we established the target performance of the NSC mortar and determined its qualitative suitability and applicability.

Table 1 Chemical composition of raw materials

Materials	Chemical composition (%)					
	SiO_2	Al_2O_3	Fe_2O_3	CaO	MgO	SO_3
OPC	15.16	4.13	3.86	67.53	3.59	3.25
GGBFS	31.08	13.66	0.49	46.79	2.55	3.05
CFA	3.80	1.32	0.51	62.05	3.34	27.55
FFA	66.49	19.21	5.08	3.86	1.50	0.48
SL	1.06	0.62	0.49	93.90	1.91	1.34

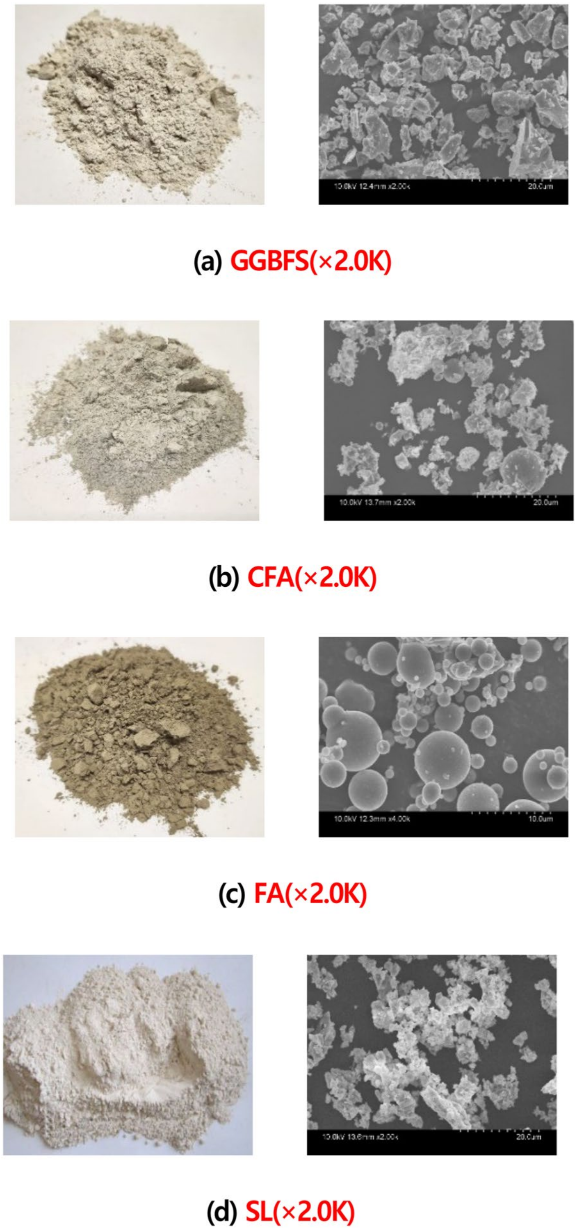

Fig. 1 Particle shape of the material

Table 4 shows the evaluation criteria for identifying the characteristics of the NSC mortar specimens. The flexural and compressive strength tests on the NSC mortar specimens that utilized 100% industrial by-products were conducted as per KS L ISO 679 Methods of testing cements—determination of strength. The flexural strength was measured using a universal testing machine (Hansin Kumpung, HST-50CS) on the specimens at the ages of 3, 7, 14, 28, and 56 days after removal of the forms. The compressive strength was measured using two cut pieces. The strength and water absorption rate were determined considering the shipment date of the PC products, and the performance was derived before and after the product age of 14 days (Ministry of Land, 2016). Additionally, scanning electron microscopy (SEM) and X-ray diffraction (XRD) analyses were conducted on the NSC mortar specimens at regular intervals.

In the water absorption test conducted on the NSC mortar specimens, the specimens were weighed in the absolute dry state, after being dried for 24 h at a temperature of 100 ± 5 ℃. The masses in the surface dry state were measured after 24 h of being submerged in clear water at a temperature of 20 ± 5 ℃. The water absorption rate W_a(%) of each specimen was obtained using Eq. (1):

$$W_a = \frac{M_1 - M_0}{M_0}, \quad (1)$$

where the weight of each specimen is expressed in the absolute dry state M_0(g) and surface dry state M_1(g).

Furthermore, to observe the internal microstructure of the NSC mortar specimens, the broken surface was obtained and fabricated in powdered form when the compressive strength of each age was measured. The sample was then immersed in an acetone solution for 1 day and observed using SEM (Hitachi, S-4800). The XRD analysis on the NSC mortar specimens was conducted under conditions of 40 kV, 30 mA, and angles of 10°–70° using an X-ray diffractometer (Diatome, MPD for bulk).

Table 2 Mixing proportions of mortar specimens

Specimen name	W/B (%)	Unit weight (g)							B:S
		Water	GGBFS	CFA	FFA	SL	OPC	Sand	
Plain	40	210	–	–	–	–	525	1,575	1:3
C5F15		210	420	26	79	–	–	1,575	
C10F10		210	420	53	53	–	–	1,575	
C15F5		210	420	79	26	–	–	1,575	
GCFS		210	420	35	35	35	–	1,575	

Table 3 Target product and KS quality standard

Target product	Flexural strength (MPa)	Compressive strength (MPa)	Water absorption (%)
Hollow blocks	–	8 ≤ S	10 ≥ A
Concrete bricks			
Ty.1[a]	–	13 ≤ S	7 ≥ A
Ty.2[b]	–	8 ≤ S	13 ≥ A
Interlocking block for sidewalk, road	5 ≤ S	–	7 ≥ A

[a] Ty.1: mainly used for outdoor or strength structure

[b] Ty.2: mainly used for indoor or non-bearing wall

Table 4 Evaluation criteria

Factors	Levels
Flexural strength (day)	Form removal and 3, 7, 14, 28, 56
Compressive strength (day)	
Water absorption (day)	3, 7, 14
SEM, XRD (day)	Form removal and 7, 14, 28, 56

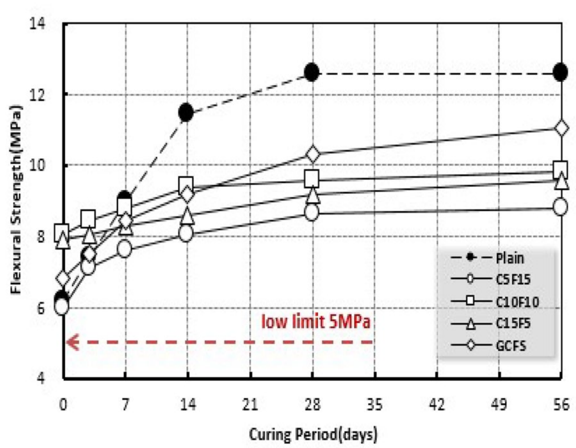

Fig. 2 Flexural strength of the mortar specimens

3 Results and Discussion

3.1 Results of Strength and Water Absorption Tests

The flexural strength test results of the NSC mortar specimens are shown in Fig. 2. As shown, the flexural strength increased with age in all specimens. The strength of de-molded plain mortar was 6.2 MPa, which was lower than that of some NSC mortar specimens. After the form was removed, the flexural strength increase was higher in the plain mortar when compared with that in the specimens, but it appeared to be insignificant after the age of 28 days.

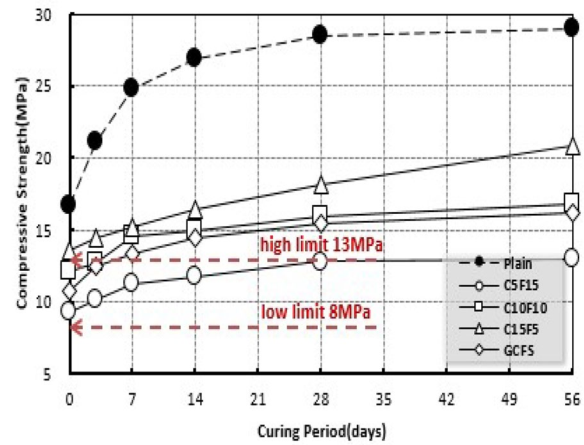

Fig. 3 Compressive strength of the mortar specimens

The strength of the de-molded C5F15 was 6.0 MPa, which was the lowest measurement recorded among all the NSC mortar specimen measurements. However, the SEM and XRD analysis results showed that the strength after de-molding increased steadily with age, whereas the flexural strength increased at a higher rate.

The strength of the de-molded C10F10 was 8.1 MPa, which was higher than that of the plain mortar, and this variant showed the best flexural strength performance among all the NSC mortar specimens. The strength of the de-molded C15F5 was 7.9 MPa, and the flexural strength increased slowly before the age of 14 days; however, it increased steadily afterward. The GCFS had a strength of 6.8 MPa after de-molding, and its flexural strength increased actively even after the age of 28 days.

The strength tests conducted on the NSC mortar specimens demonstrated that all the specimens met the target flexural strength performance of 5.0 MPa. Furthermore, in terms of the required strength characteristics of PC, C10F10 was deemed the most suitable. Additionally, the NSC mortar specimens demonstrated a steady increase in flexural strength and sustained a stable hydration reaction even after the age of 14 days, when compared with the plain mortar.

Figure 3 illustrates the results of the compressive strength tests conducted on the NSC mortar specimens. As shown in the figure, the compressive strength increased with age in all specimens. C5F15 exhibited a tendency similar to that of the flexural strength test results. When the form was removed, the compressive strength was 9.3 MPa, which was the lowest measurement among all the NSC mortar specimen measurements. However, the compressive strength demonstrated a steady increase even after the age of 14 days. C10F10 showed a strength of 12.1 MPa after de-molding, which increased steadily in the compression strength tests even after the form removal. The compressive strength at the age of three days satisfied the structural standards of the target products, and the strength performance was maintained even after the age of 14 days. C15F5 exhibited the highest degree of strength after de-molding among the NSC mortar specimens, with a compressive strength of 13.6 MPa after the form removal. Similar to the case of C10F10, the structural standards of the target products were met here too at the age of three days.

The compressive strength increased gradually and exhibited the highest increase after 28 days. Thus, the compressive strength of the mixture is expected to improve on a long-term basis. The compressive strength of GCFS was 10.7 MPa after the form removal, and the structural standards of the target products were met after the age of 7 days. The compressive strength analysis of the NSC mortar specimens demonstrated that all mixtures met the minimum target performance of 8.0 MPa. The compressive strength measurements appeared lower compared with those of the plain mortar; however, the structural standards of the target products were met in some mixtures. The NSC mortar specimens also demonstrated the capability to maintain a stable target performance even after the standard age of 14 days. Hence, steam curing resulted in the NSC mortar specimens achieving initial strength, following which improvement in soundness and long-term strength was observed. Additionally, the NSC mortar specimens met most of the strength performance standards of the target products presented in Table 3. At the age of 14 days, the flexural and compression strengths were the highest at CFA:FFA = 1:1 and CFA:FFA = 3:1, respectively.

Figure 4 illustrates the water absorption rates of the NSC mortar specimens.

As shown in the figure, the water absorption rates decreased with age in all specimens. The water absorption rate of the plain mortar was 6.5% at the age of 14 days and was very low when compared with those of the NSC mortar specimens.

The NSC mortar specimens showed the lowest water absorption rate standard of 13% or less in all mixtures, and the structural standards of the target products in C10F10 and GCFS were met at the age of 14 days. C10F10 and C15F5 also exhibited compressive strengths exceeding 13.0 MPa at the age of 14 days; however, C10F10 was deemed the most suitable specimen considering durability-related water absorption capabilities. While C15F5 showed the highest compression strength among all the NSC mortar specimens, it also had the highest water absorption rate. This tendency can be inferred as the durability degradation caused by the concentration of the internal C15F5 microstructure with needle-like hydration products. Moreover, GCFS using SL was also observed to meet the structural standards of the target products. Because SL is more economical and safer to handle than alkaline activators are, it is mainly used as a stimulant for industrial by-products-based binder materials and functions as a substitute for alkaline activators. The mixture proportion of GCFS was CFA:FFA:SL = 1:1:1, whereby a stable water absorption rate was shown among the NSC mortar specimens. However, as the target strength of C10F10 and C15F5 was revealed faster than that of SL-substituted mixtures, the quality standards of the concrete products were met without using SL.

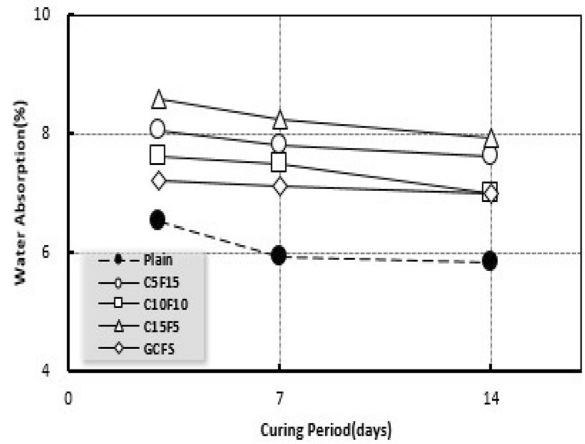

Fig. 4 Absorption factor of the mortar specimens

The strength test results and water absorption rates at the standard age demonstrated that C10F10 was the most suitable fit, and that the optimal CFA to FFA ratio was 1:1. However, when the structural parts are applied, a further evaluation of the durability supplement is required when the PC products are shipped before the age of 14 days.

3.2 XRD and SEM Analysis

Figure 5 illustrates the XRD analysis results pertaining to the NSC mortar specimens. The main mineral components were quartz (SiO_2), portlandite ($Ca(OH)_2$), and calcite ($CaCo_3$). For the plain mortar (Fig. 5a), the high peaks associated with $Ca(OH)_2$ generation were observed near 8°, 34°, 47°, and 51° (2θ). In this case, when the hydration reaction of OPC progresses adequately, $Ca(OH)_2$ generation is active, and the internal microstructure is dense (Park et al., 2018). Therefore, it is believed that the plain mortar exhibits outstanding strength and water absorption (Na et al., 2020).

In the NSC mortar specimens using CFA as a stimulant, hydration products (i.e., ettringite and C–S–H) were

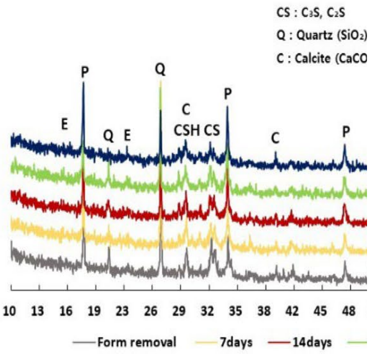

(a) Plain

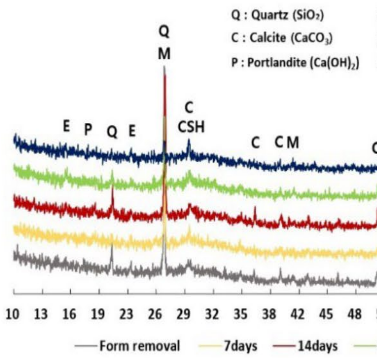

(b) C5F15

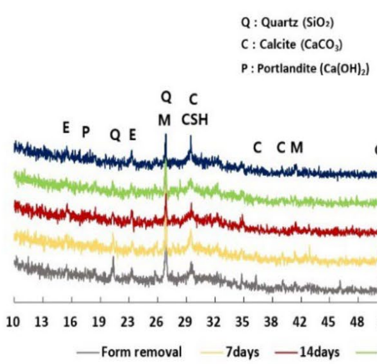

(c) C10F10

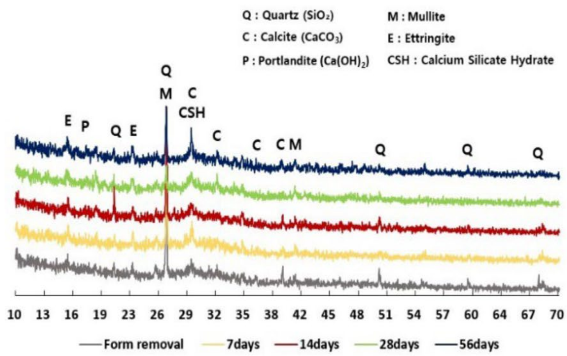

(d) C15F5

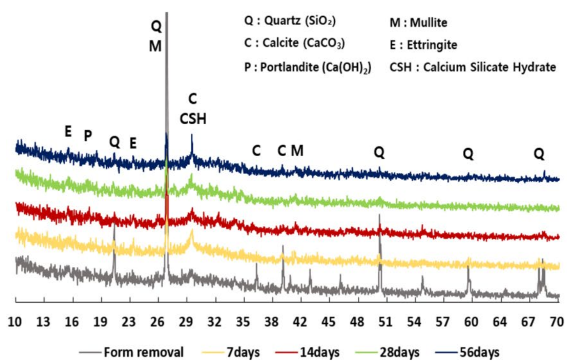

(e) GCFS

Fig. 5 X-ray diffraction analysis

observed. Additionally, as the substitution of CFA increased, the peak of the hydrates became sharper and clearer. This behavior was owing to CaO, the main component of CFA. Specifically, CaO in the NSC mortar specimens combines with moisture to create $Ca(OH)_2$ and elutes SiO_2 and CaO contained in GGBFS. This was confirmed via the XRD analysis of each mixture when the forms were removed.

Accordingly, the NSC mortar specimens were observed to form a dense internal structure through a calcium silicate hydration reaction. Moreover, whereas the NSC mortar specimens showed different variations for each mixture, the quartz and portlandite peaks generally reduced with age, unlike those of the calcite and C–S–H that increased with age. This behavior was owing to the stabilization of hydration products. That is, ettringite with a low crystalline structure improves in strength through a dense internal structure by forming a highly crystalline C–S–H (Park, 2013).

Figure 6 illustrates the internal microstructure observation of the NSC mortars obtained using SEM. The NSC mortar specimens were promoted with a hydration reaction through steam curing, allowing for the identification of hydrates such as ettringite and C–S–H when the forms were removed, and the internal structure gradually appeared dense with age.

Additionally, with age, the NSC mortar specimens were integrated into a laminated form of hydrates, which appeared to cause expansion cracks owing to rapid hydration reactions. This phenomenon is also considered to cause the higher water absorption rate of NSC mortar when compared with that of plain mortar.

In the plain mortar (Fig. 6a), plate-shaped hydrates seen as $Ca(OH)_2$, with a dense, stable internal surface, were observed. In the NSC mortar specimens (Fig. 6b–e), shapes with net-like connections of needle-like products were observed at an early age. This internal structure can be disadvantageous in terms of compression strength and water absorption rate; however, it contributed to a higher flexural strength performance than that of plain mortar at an early age. It was further observed that the internal structure was closely coupled via generation of hydrates between needle-like structures. This is believed to have resulted in the stable performance of the NSC mortar specimen.

In C5F15, a stabilized internal surface was observed at the age of 28 days, whereas this was observed from the age of seven days in C10F10. As the reactivity varies

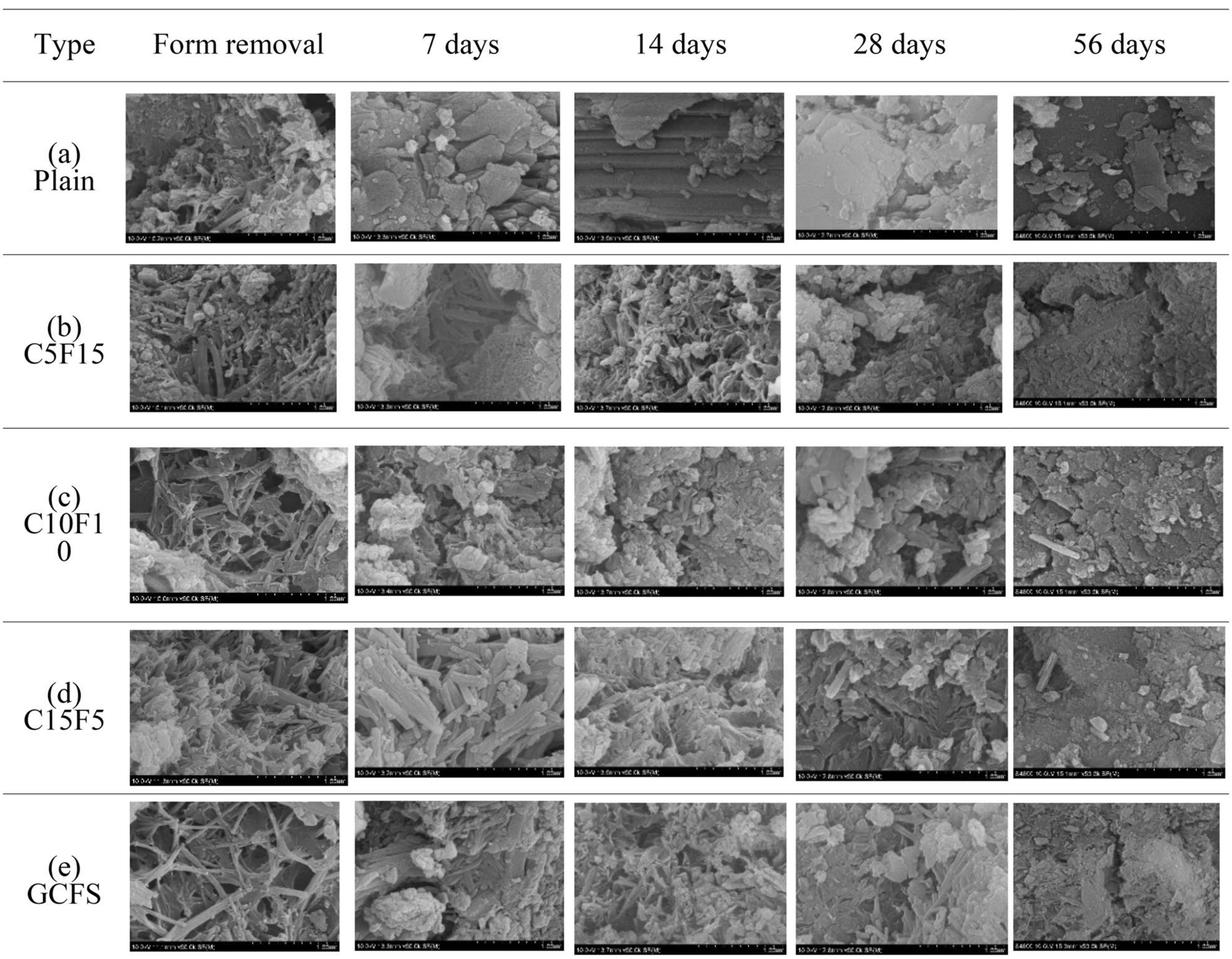

Fig. 6 SEM images

depending on the substitution ratio of the materials, the dynamic performance of each mixture also differs. Among the NSC mortar specimens, C15F5, which showed the highest hydration reaction, appeared to be a mixture of several hydrates from the beginning of the form removal; nevertheless, several micro-cracks were observed until the age of 28 days. Therefore, C15F5 is believed to exhibit a high water absorption rate owing to the expansion cracks. As GCFS tended to form hydrates reliably, the internal structure was tightly integrated.

4 Conclusions

This study aimed to investigate the suitability of NSC mortar based only on industrial by-products for creation of PC products. Moreover, the characteristics of the NSC mortar were assessed according to existing quality standards. Our major findings can be summarized as follows:

1. The NSC mortar satisfies the quality standards prior to the standard age as a result of steam curing, and it will be highly useful as raw material for target products.
2. The NSC mortar specimens meet both the strength and water absorption standards of existing PC products.
3. The NSC mortar specimens form a dense internal structure through the calcium silicate hydration reaction.
4. Although expansion cracks are observed, the NSC mortar specimens gain strength at an early age following steam curing. However, depending on the substitution ratio of the materials, the mortar specimens display different reactivities; hence, stable internal structures are observed in some specimens.

The appropriate mixing proportion applicable to production materials of the target PC products was derived to be C10F10 (CFA:FFA = 1:1). The NSC mortar developed in this study provides a suitable option and developmental basis for non-sintered binder materials. To increase its utilization throughout the construction industry in the future, it will be necessary to complement its strength and durability. Hence, further studies are required to verify the usability of the products under on-site conditions.

Acknowledgements
Not applicable.

Author contributions
H.N.: conceptualization conceived and wrote the manuscripts, analyzed the data. W.H.: advice and revised the manuscript. All authors agreed with the final version of the manuscript.

Funding
This work was supported by the National Research Foundation of Korea(NRF) grant funded by the Korea government(MSIT) (No. 2023R1A2C2003956).

Availability of data and materials
All data generated or analyzed during this study are included in this published research.

Declarations

Competing interests
The authors declare that they have no competing interests.

Received: 3 January 2024 Accepted: 14 April 2024
Published online: 01 August 2024

References

Korean Agency for Technology and Standards Homepage. (2023). KS L 5405: Fly ash. https://e-ks.kr/streamdocs/view/sd;streamdocsId=72059226396331171. Accessed on December 4, 2023.

Korea Ministry of Environment. (2019). National greenhouse gas inventory report of Korea, Greenhouse Gas Inventory and Research Center, Korea, 11-1480906-000002-10, 15-169, www.gir.go.kr/home/index.do?menuId=36 **(in Korean)**.

Lee, S. H. (2017). Revised provision of KS L 5405 Fly Ash for CFBC fly ash to applying concrete. *Magazine of RCR (Journal of the Korean Recycled Construction Resources Institute), 12*, 20. https://doi.org/10.14190/MRCR.2017.12.2.020

Ministry of Land, Infrastructure and Transport. (2016). *Korean Construction Specification Precast Concrete*, KCS 14 20 52, 8.

Na, H. W., Moon, K. J., & Hyung, W. G. (2020). Application of precast concrete products of non-sintered cement mortar based on industrial by-products Journal of the Korea Institute of Building. *Construction, 20*, 19–26. https://doi.org/10.5345/JKIBC.2020.20.1.019

Park, J. W., Kim, J. H., Lee, M. H., & Chung, C. W. (2018). Carbonation mechanism of hydrated cement paste by supercritical carbon dioxide. *Journal of the Korea Institute of Building Construction, 18*, 403–412. https://doi.org/10.5345/JKIBC.2018.18.5.403

Park, S. G. (2013). Reaction characteristics of non-cement mortar using ground granulated blast furnace slag. *Journal of Korea Contents Association, 13*, 393–399. https://doi.org/10.5392/JKCA.2013.13.09

Shin, G. S. (2020). *Assessment on reaction characteristic and durability of ambient cured geopolymer concrete incorporating GGBS*. Ph.D. Thesis, Kangwon National University, Chuncheon, Korea. https://m.riss.kr/link?id=T15470650

Publisher's Note

Hyeong-Won Na earned a Ph.D degree in Architecture Engineering(Architecture Materials) from YeungNam University. She currently runs an eco-friendly construction materials research center. She mainly works on ecofriendly cement and concrete.

Won-Gil Hyung is a professor at the Department of Architecture at Yeungnam University. He is researching various building materials. Recently, he has been researching eco-friendly cement and resource-recycling concrete.